Strategies in cone beam CT inspection of cylindrical objects

Wannes Goethals[1], Marjolein Heyndrickx[1], Matthieu Boone[1]

[1]UGCT-Department of Physics and Astronomy, Proeftuinstraat 86, 9000 Ghent, Belgium
e-mail: wannes.goethals@ugent.be, marjolein.heyndrickx@ugent.be, matthieu.boone@ugent.be

Abstract

Axial symmetry is a feature that often occurs in industrial parts. Analysing these with X-ray computed tomography (CT), cylindrical coordinates about an axis fixed to the object form the most natural base to check certain characteristics of objects that contain such symmetry. This work presents two methods to investigate this coordinate system and to incorporate it in the current algebraic reconstruction framework and the analysis tools. The methods are applied to fast scans with few projections of cylindrical products with slight random tilts. Standard reconstruction requires more advanced and hence slower techniques in the analysis phase. Reconstruction in a symmetry adapted base needs precise knowledge about the object's pose, but it allows aimed sampling. This takes down the reconstruction and analysis time, which is necessary when applying CT for in-line inspection.

Keywords: cylindrical coordinates, cone-beam X-ray computed tomography (CT), algebraic reconstruction, 3D analysis

1 Introduction

In modern day industry, the newly manufactured products are becoming more complex while quality and production rate requirements keep increasing. That's why Non-Destructive Testing (NDT) is a growing field in medical technology, aerospace, agricultural sectors etc. Common non-destructive methods like radioscopy, ultrasound, optical or thermal imaging are used in different sectors such as material characterization or production control [1].

As the industry is gradually becoming aware of the options that X-ray CT offers as a non-destructive 3D inspection tool, this leads to the demand for systems specifically designed for scanning sequences of same-type objects in a high throughput environment. The challenges lie in the fact that a variety of factors restrict the number of projections to *as low as technically feasible*. The solutions can be found in more advanced reconstruction techniques. Even though iterative reconstruction can't compete with the analytic counterparts in terms of reconstruction time (for standard cone-beam geometry), they allow making fewer projections with still reasonable results by incorporating prior knowledge. This reduces the scan time and the absorbed radiation dose per object.

Previous studies have shown that iterative reconstruction schemes using cylindrical coordinates can alleviate memory requirements and be less subject to noise than Filtered Back-Projection (FBP) algorithms [2]. As a negative point of attention, Jian et al. [3] reported a loss in resolution due to non-uniform sampling. In these studies, the cylindrical coordinate axis is positioned along the vertical axis of the rotation stage. When this axis is perfectly centred on the field of view origin, some very specific acceleration schemes can be applied. This requirement is met in circular cone beam CT, which is the standard in research environments.

In this work two strategies for batch CT inspection of cylindrical objects are presented. First the common goals will be explained in detail. The two distinct strategies will be presented in parts 2.1 and 2.2. In 2.3 the inspection tests will be briefly summarized.

2 Methods

When analysing cylindrical objects, the most convenient space to work in is a cylindrical coordinate system positioned along the symmetry axis of the object. The goal of each strategy is to reconstruct the given projections to this space with optimal quality. In general the object won't be perfectly aligned with the rotation axis of the CT scanner, so 3D pose estimation must be performed before transforming to cylindrical coordinates. The object pose can be captured in six degrees of freedom. Three intrinsic *zxz* Euler angles are captured in the rotation matrix R, while T translates the object along the three spatial coordinates:

$$X' = RX + T \tag{1}$$

After the alignment to (x', y', z') in equation (1), a transformation to cylindrical coordinates around the z'-axis is performed on this oriented set of coordinates. This is visualised in figure 1.

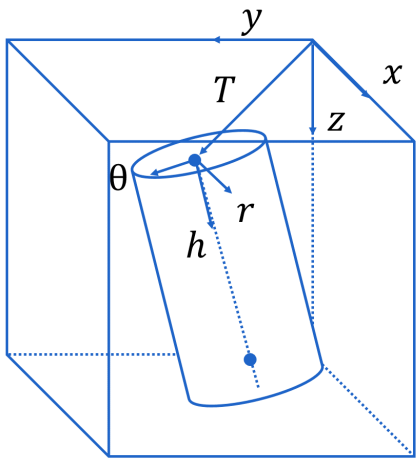

Figure 1: The cylinder can take a free pose in the scanning space.

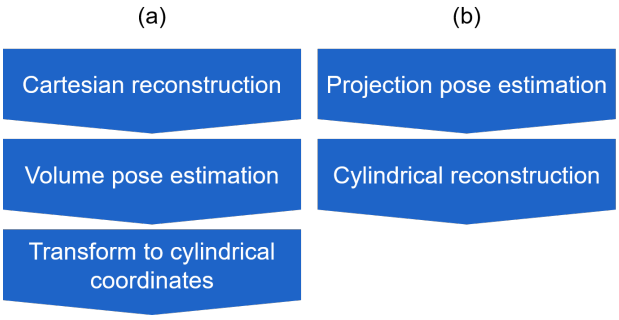

Figure 2: Two strategies to transform the projections to a reconstruction along the symmetry axis of the scanned object.

$$\begin{cases} r = \sqrt{x'^2 + y'^2} \\ \theta = \arctan\left(\dfrac{y'}{x'}\right) \\ h = z' \end{cases} \tag{2}$$

A common fault case in a production environment is the situation where a component is missing in an assembled product. When the components are obscured from visual inspection, an X-ray CT scan may offer better insight on manufacturing quality. To illustrate how the developed strategies can be applied in a real production environment, a batch of 50 medical safety needles with artificially induced internal defects was provided by a manufacturer. High-detail scans were made in-house in the initial phase to characterize the reconstructed objects (see table 1 for details). A working demonstrator has been made by XRE NV and used to perform the series of high-speed scans (table 2).

Table 1: Imaging parameters for the precision scans of the medical device

Geometry	Circular cone beam			
	Source Detector Distance	SDD	1062.09	mm
	Source Object Distance	SOD	186.16	mm
	Number of projections	N_p	1201	
	Last scan angle		360°	
Detector	Perkin Elmer 1620			
	Detector size (ROI)	H, W	$2000, 600$	
	pixel size	p_d	0.2	mm
	exposure time	t_{exp}	1000	ms
Reconstruction 1	Cartesian SART			
	voxel pitch	p_v		
	relaxation	λ	0.15	
	shape	N_z, N_y, N_x	$1991, 600, 600$	
Reconstruction 2	cylindrical SART			
	shape	N_h, N_θ, N_r	$1982, 1730, 275$	

2.1 Cartesian reconstruction and posterior pose estimation

The first strategy is shown schematically in figure 2(a). It starts with a standard Cartesian reconstruction, from which a cylindrical shape is extracted. Equations 1 and 2 can then be used to transform the reconstructed image.

Figure 3(a) shows a slight tilt of the object, which is even present in a high-quality scan. Usually this doesn't carry the highest priority, as it may take some time to centre the sample manually with this precision. But when cylindrical transformation is carried

Table 2: Imaging parameters for high speed circular cone beam scans of medical devices

Geometry	Circular cone beam			
	Source Detector Distance	SDD	791	mm
	Source Object Distance	SOD	679	mm
	Number of projections	N_p	21	
	Last scan angle		200°	
Detector	Varex 1512			
	Detector size	(H,W)	(1536,1944)	
	Detector pixel size	p_d	0.748	mm

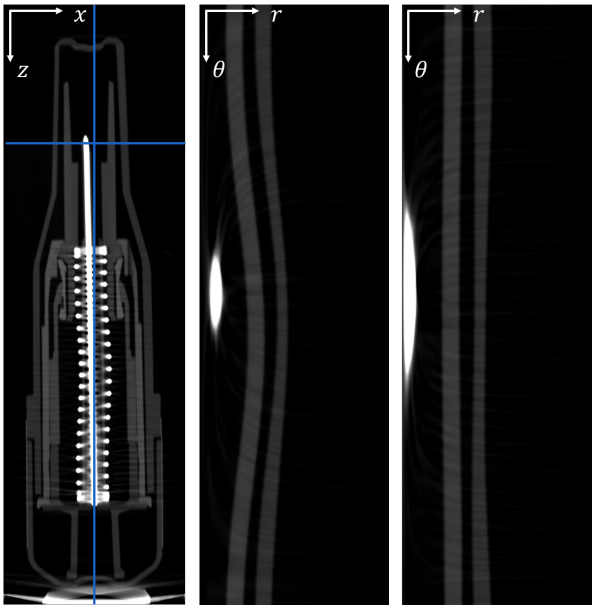

(a) (b) (c)

Figure 3: The central xz slice (a) shows a slight tilt of the object w.r.t. the central z axis. Naive transformation to cylindrical coordinates introduces unwanted deformations in (b). (c) is the result of better alignment

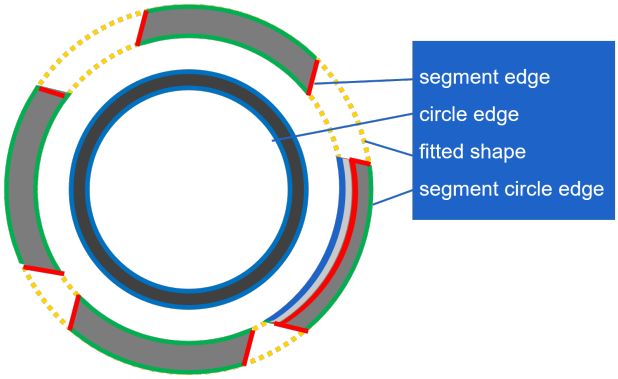

Figure 4: Schematic reconstruction based cylinder pose estimation. Only the real circle edges of the wanted segment, in this case the outer ring structure, are kept to estimate the pose.

out w.r.t. the central z axis, unwanted deformations will affect the inspection measures. Circular objects won't become regular in the new coordinate space, but will be deformed as shown in figure 3(b). This disturbs further analysis in an uncontrollable way. To retrieve the cylinder pose, some image analysis needs to be performed on the reconstruction. In figure 4 a sketch is made to summarize the segmentation steps. Best results are obtained when false edges are kept to a minimum. Only pixels with a sufficient radial gradient from the centre are used. This assumes the object is already approximately centred. This approach reduces the influence of radial streaks coming from metal components or due to aliasing artefacts. The edges that look circular preferably originate only from one segmented cylindrical object. A single or dual threshold technique extracts the wanted component, after which a binary edge filter is applied. Notice in figure 3(a) how some components don't have a mutual symmetry axis. It is best to extract the most stable component to which others are optimally aligned. Eventually only the pixels that are both circle edges and segment edges are kept to extract the cylindrical shape. A randomized Hough transform based on [4] calculates the rotation and translation needed in equation 1.

2.2 Prior pose estimation and cylindrical reconstruction

The second strategy is to perform prior pose estimation of the object. A brief summary of existing techniques for general shape surface pose estimation can be found in [5]. A method has been developed to derive the object's pose directly from the projected images. This can be done very efficiently due to the axial symmetry of the object. With this prior info, a reconstruction in cylindrical space along the object can be performed. This method allows more advanced reconstruction techniques that incorporate structural information of the object. Analysis can be executed directly in this space.

The idea of the projection based pose estimation is to trace back the coordinates of projected points to 3D volume space as

the intersection of rays. Minimally two views from different projection angles are needed, yet using more views increases the stability. Two 3D points along the axis are sufficient to fix 5 degrees of freedom. A practical implementation is illustrated in figure 5. The most stable symmetric feature is segmented by threshold and dilation techniques. Then the pairwise centres of the four corner pixels are assumed to be on the symmetry axis.
The internal central part coloured green has an intermediate projected grey value. Anything darker or brighter is excluded. Problems arise at the edges of the dark objects. In this image, the needle, spring and object holder at the bottom are coloured red. At the edges where they have less material to attenuate the X-rays, the grey values are equal to the ones of the central part. Binary dilation of the red parts exclude this error. Similar issues are present in the blue area due to the sample holder. This is simply excluded by setting a vertical coordinate threshold below which everything is excluded. When intensity variations of the detector corrupt the segmentation completely, the median absolute deviation method by [6] points out unnatural jumps in the position changes. Then these projections are excluded from the coordinate backtracking algorithm.

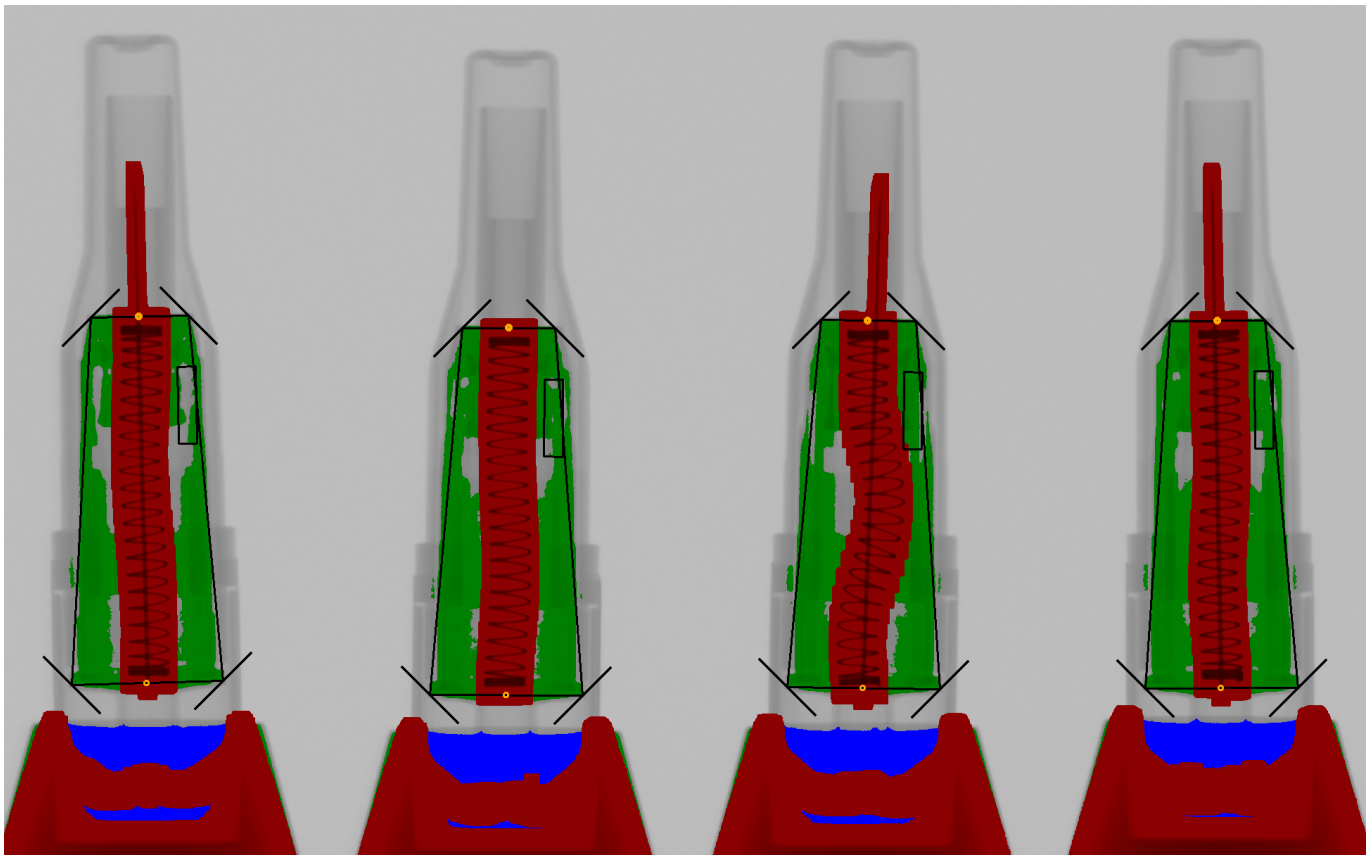

Figure 5: Basic segmentation methods are sufficient to find the projected symmetry of the objects

When the pose of the object is found, a modified Simultaneous Algebraic Reconstruction Technique (SART) algorithm [7, 8] is used to reconstruct the scan to cylindrical coordinates fixed to the tracked object. Standard methods use Cartesian coordinates centred on the rotation stage axis. This modification allows to incorporate more prior information in the reconstruction algorithm. In this case the components show little to no variation in the azimuthal direction. This info can be included to choose the number of voxels in each reconstruction direction. The most common polar division policy uses a constant number of radial (N_r) and azimuthal (N_θ) voxels. The azimuthal spacing increases linearly with the radial position in this way. Other than that, this constant N_θ can be chosen to be any arbitrary integer number, depending on the number of details in this direction. Analogous arguments apply to the other symmetry directions.
To assess the quality of the cylindrical method, a high-precision scan is performed (see table 1 for details). This is reconstructed with the Cartesian and the cylindrical method. The first reconstruction is transformed afterwards to the cylindrical frame using the same pose estimation to rule out any influence by this aspect. Reconstruction times are recorded as these are an important limitation to high-speed applications.
The Cartesian and cylindrical reconstruction are also compared for the high-speed scans (table 2). Grids of $(N_z, N_y, N_x) = (240, 120, 120)$ and $(N_h, N_\theta, N_r) = (240, 40, 60)$ are used. These have the same sampling rate in height and radial direction. The number of voxels is kept low, considering the low amount of projections. The detector does have a good spatial resolution compared to the number of projections, seeing that the projected object width is about 260 pixels. However no one-to-one

correspondence to N_θ or N_r can be made.

2.3 Developments of tests in cylindrical coordinates

To illustrate the advantages of the symmetry adapted base, some inspection tests will be presented. These are developed specifically for the scanned product, but some concepts can be extended to any object with cylindrical symmetry. Only a few orthogonal views are needed to spot a variety of defects. Three classes of defects can be distinguished in the used samples. Components can be either missing, moved or deformed.
The tests are developed on the batch scan of 50 products. As they are artificially introduced, it is known by the manufacturer what defect is present in each product. This allows any fine-tuning to maximize the tests' sensitivities and accuracies. In this batch, 10 defect cases are artificially introduced to explore the capabilities of fast X-ray CT inspection. Only four of these will be explained in detail as they cover the three classes of defects sufficiently.

In figure 6 three reconstructions can be observed, averaged over the azimuthal dimension. When no information on the internal rotation is present, this averaged view can already be a first indication that a defect has occurred. A key component, with a ring shape in Cartesian space, indicated by the red rectangle is either missing or has moved in figures 6(b) and (c). A simplified template matching technique will tell where the component is located if it is present. This is a standard type of internal defects.

From the sample position, it is known at which radius and height the ring should be located in the view. No rotation or scaling can be present. The position is retrieved by initially reducing the red rectangle area to a vertical line profile of its maximal grey values at each height. A subsequent sliding window average of these maxima in the axial direction yields the starting height of the ring and tells if it is present.

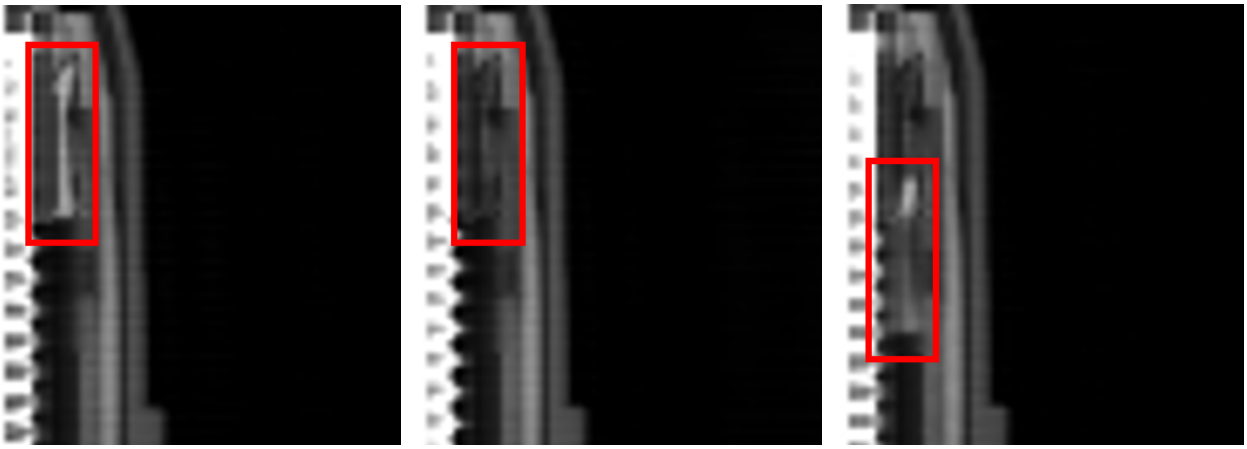

(a) (b) (c)

Figure 6: A cropped *rh* slice averaged over θ for three different samples. In (a) no defect is present. In (b) a piece is missing and in (c) the piece has been moved to a different location.

Similar methods are used to inspect the spring area. There's little need to have information in the azimuthal direction, so the average view can be reused to optimize for speed. Two types of defects have been introduced here. As shown in figure 7, the spring be either dilated in the axial direction or have an abnormal width. All voxels in the broad spring area above the median value are thresholded as part of the spring. The maximal radius indicates a missing guide for the spring, as shown in figure 7(c). A sliding window average similar to the one presented for the ring test indicates a gap when the spring is dilated.

3 Results

For the scan described in table 1 the first and second reconstruction are compared. When an equal amount of voxels is used ($N_\theta = 1315$ instead of $1730 \approx 2\pi \cdot 275$) the total reconstruction time is 405s compared to 354s for the Cartesian case. The time increase of 14.4% comparing with the Cartesian method can be attributed to the intermediate coordinate transformations.
The differences are shown in the latter coordinate frame in figure 8 by performing a base transformation of the Cartesian reconstruction. Quantitatively, the attenuation coefficients are similar, only at the edges some differences can be observed. This can be either due to sampling artefacts in the transformation of the Cartesian result or due to the cylindrical method of reconstruction. Intermediate clipping explains the zero difference at the highly attenuating part. The right half of the difference figure hints at a misalignment issue, while this isn't clear in the left part. No misalignment was expected as the same transformation matrices

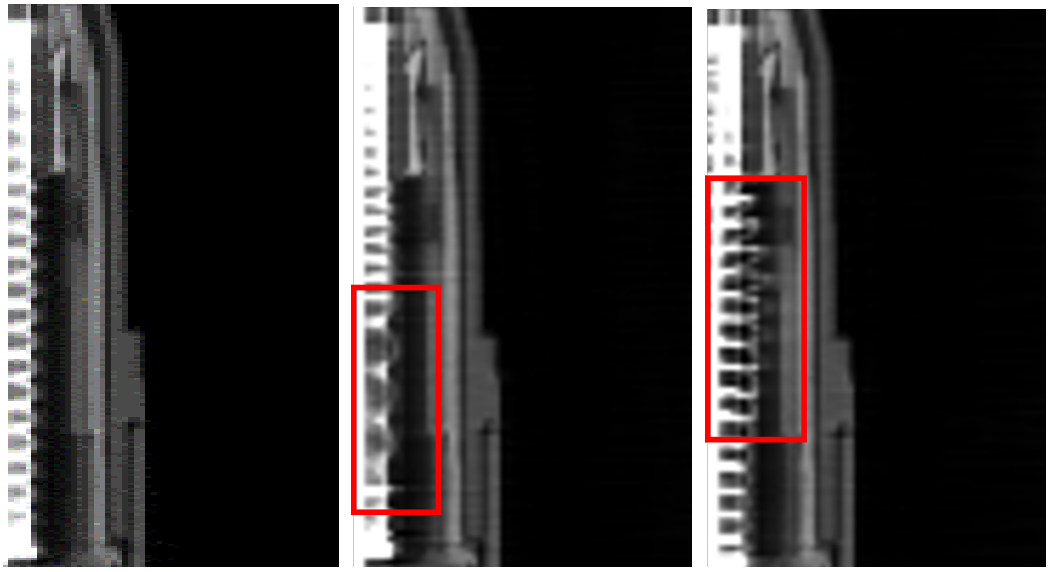

(a) (b) (c)

Figure 7: A cropped *rh* slice averaged over θ for three different samples. In (a) no defect is present. In (b) a spring dilated in the axial direction has been introduced and in (c) a spring guide has been removed, which is seen in the wide path of the spring.

have been used. Next to that, some characteristic metal streaks can be observed in this figure. These are present in both types of reconstruction.

From this test, one can conclude that when a scan has been performed with optimal parameters, no significant improvement or decline of reconstruction quality can be observed. In fact, the algorithm takes 14.4% more time compared to the Cartesian method when an equal number of voxels is used. The improvement is situated mainly in the case of a high-speed scan. Then the number of voxels can be dropped in the symmetry directions tied to the object. The number of azimuthal voxels N_θ should be in the order of the number of projections N_p to reduce aliasing artefacts. Taking this into account, the reconstruction time drops severely and more accurate results can be obtained. To approach the slow scan quality, more advanced reconstruction techniques are required though.
The reconstructions mentioned at the end of subsection 2.2 take on average 0.30s for the cylindrical case. The Cartesian reconstruction time takes 1.53s as more voxels are required to reach the same radial sampling rate. These values lie in the line of expectation, comparing with the previous result: a factor of 6 decrease in number of voxels for the cylindrical reconstruction, but 14.4% more time due to intermediate transformations. In figure 9 the two can be compared visually, in both cases a reconstruction of two iterations with a relaxation factor of 0.5. Scan times are currently 13.9s between the first and 21st projection.

In 9(a) the radial streaks make it difficult to retrieve the pose from the reconstructed image. The second strategy has a good alignment, apparent in the figure where all cylindrical features centred on the axis become rectangular. Since the goal of the research is to apply it to high-speed scans, the first strategy is no longer developed as more advanced techniques would be needed and the second strategy gives precise results for every single scan. 3D rigid registration with a preloaded scan would probably yield a fine estimate but these techniques require more processing time. With prior pose estimation, good precision can in theory be attained from as few as two projections.

For eight out of ten defects, the tests start to develop a clear distinction between the control group and the samples with the respective introduced defects. Two features can't be spot at the reconstructed resolution. In the first, a small corner has been chipped off. Objects with the second bug have lost strength due to a brief reversible high deformation. This leads to no density change or final deformation which makes it impossible to notice with absorption CT. Further developments are required on the second reported strategy to acquire robust in-line CT inspection. The total processing (loading of images, pose estimation, reconstruction and analysis) covers on average 1.64s per scan.

4 Conclusion

Two strategies have been developed to transform scans with few projections to a reconstruction in the symmetry base of the objects. In this adapted coordinate system, a number of tests have been developed to indicate defective products.

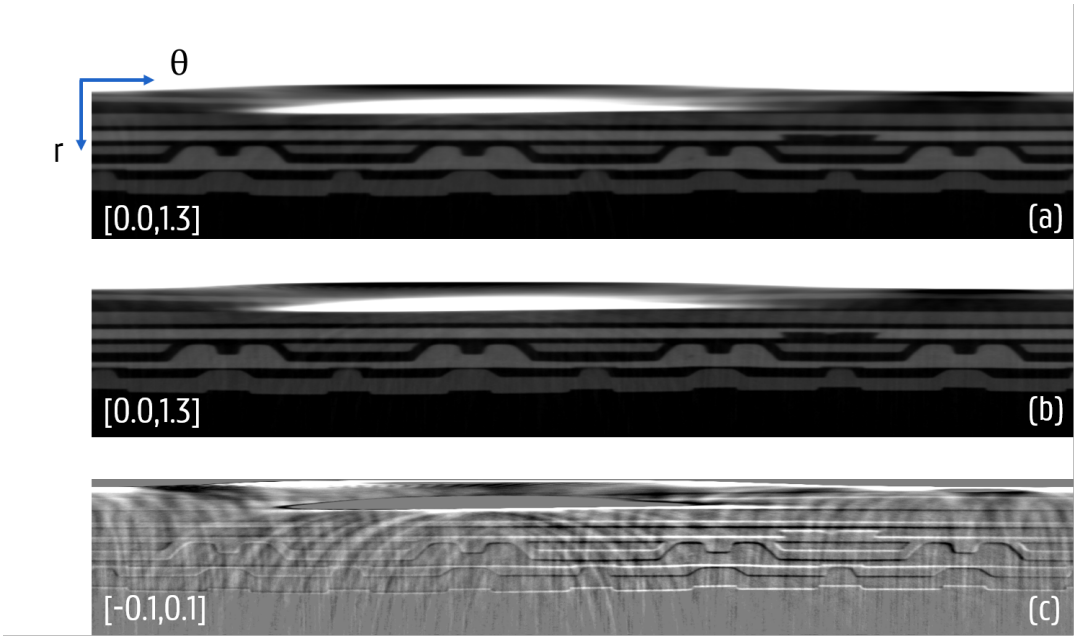

Figure 8: The top figure (a) shows a Cartesian reconstruction slice that's been transformed to a θr frame. (b) Shows a direct reconstruction in cylindrical coordinates. The difference (a) - (b) between these in (c) shows some effects at the edges. Some deformed streaks can be noted as well. The grey value ranges are expressed on the left in units cm^{-1}.

The first strategy eventually hasn't been successful as the volumetric pose estimation suffered badly from the poor reconstruction quality. Edges are too unclear due to the low number of projections. Other techniques might require too much processing time. The projection based pose estimation technique yields persistently good results. This is embedded in the second strategy with subsequent cylindrical reconstruction in the object's space. This kind of reconstruction allows for aimed resampling, so less time is required to reconstruct the internal structure. In this case the total processing time of the scans is on average 1.64s per sample. More advanced techniques can be included to improve reconstruction quality as the coordinate system is attached to the object. In the same scope, a paper on the use of an initial volume and weighted back-projection in cylindrical coordinates is in preparation. The analysis phase can be started immediately in a suited coordinate system, so less time-consuming methods can be used. Based on a comparison of two distinct methods and a following test phase, this method proves to be viable for high throughput CT inspection of axial symmetric components. This will improve the fraction of manufactured objects that satisfy safety and quality requirements.

Acknowledgements
This research is funded by the imec ICON project iXCon (Agentschap Innoveren en Ondernemen project nr. HBC.2016.0164). The work by M. Heyndrickx was funded by the Research Foundation Flanders (FWO) [grant number 1S 215 16N].
The authors would like to thank the manufacturer for providing the samples with introduced faults and also XRE NV for acquiring part of the projection data (`www.xre.be`).

References

[1] R. Hanke, T. Fuchs, N. Uhlmann, X-ray based methods for non-destructive testing and material characterization, Nuclear Instruments and Methods in Physics Research Section A: Accelerators, Spectrometers, Detectors and Associated Equipment 591 (1) (2008) 14–18.
[2] Thibaudeau Christian and Leroux Jean-Daniel and Fontaine Réjean and Lecomte Roger, Fully 3d iterative ct reconstruction using polar coordinates, Medical Physics 40 (11) (2013) 111904.
[3] L. Jian, L. Litao, C. Peng, S. Qi, W. Zhifang, Rotating polar-coordinate art applied in industrial ct image reconstruction, NDT&E International 40 (4) (2007) 333 – 336.
[4] R. A. McLaughlin, Technical report-randomized hough transform: Improved ellipse detection with comparison, University of Western Australia.
[5] L. F. Rocha, M. Ferreira, V. Santos, A. P. Moreira, Object recognition and pose estimation for industrial applications: A cascade system, Robotics and Computer-Integrated Manufacturing 30 (6) (2014) 605–621.
[6] B. Iglewicz, D. C. Hoaglin, How to detect and handle outliers, Vol. 16, Asq Press, 1993.
[7] T. De Schryver, Fast imaging in non-standard x-ray computed tomography geometries, Ph.D. thesis, Ghent University (2017).

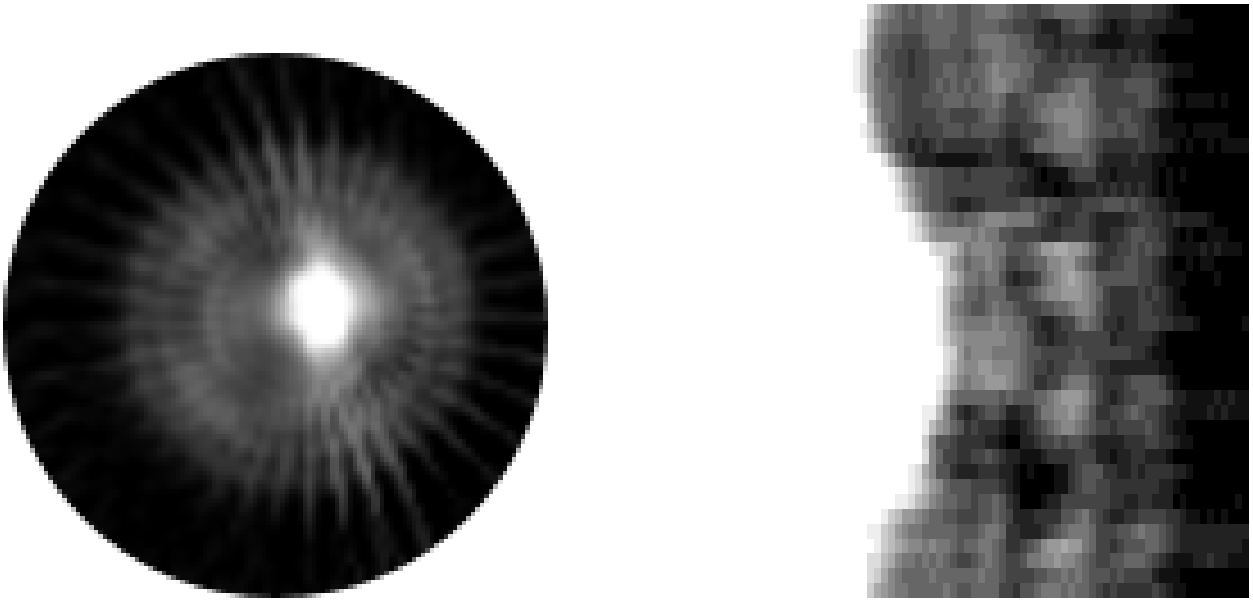

(a) (b)

Figure 9: A horizontal slice of a Cartesian (a) and a cylindrical (b) reconstruction. (a) shows some radial streaks, whereas (b) has fewer due to the low azimuthal sampling rate.

[8] W. Goethals, M. Heyndrickx, M. Boone, An iterative cylindrical reconstruction algorithm aligned with the object for fast x-ray tomography (in preparation).